STUDY OF A STRONG RFI SOURCE AT L-BAND USING SMAP RADIOMETER DATA

Paolo de Matthaeis[1,2], David M. Le Vine[1], Yan Soldo[3], Alvaro Llorente[4]

(1) NASA Goddard Space Flight Center, USA
(2) Universities Space Research Association, USA
(3) ESA/ESTEC, The Netherlands
(4) ESA/ESAC, Spain

ABSTRACT

This paper presents an analysis of Radio Frequency Interference (RFI) in the 1.400-1.427 GHz frequency band. The study considers the sudden and strong increase of interference from a particular emitter in China that has been observed in July 2020 by radiometers from both ESA's SMOS (Soil Moisture Ocean Salinity) and NASA's SMAP (Soil Moisture Active Passive) missions. It provides an example of the characterization of a source of RFI and illustrates the capabilities of the SMAP radiometer receiver and RFI processing incorporated in it to identify and understand interference.

Index Terms— Radio Frequency Interference, SMAP, L-band radiometry.

1. INTRODUCTION

The source of the interference has been located East of the Chinese city of Hangzhou in an area with radar installations. RFI is unfortunately rather common over China and interference originating from this location has been observed by SMOS and SMAP for some time. However, in July 2020 the level of radiation increased dramatically reaching levels of 1,000,000 K as reported by SMOS. Several features of SMAP helped provide insight into the source. In addition to the conical scan, which enables location, SMAP provides high temporal resolution and spectral analysis (16 channels across the protected band). This paper will report an analysis of this very strong source (a radar). It provides an example of a well defined source of RFI and illustrates the power of the SMAP radiometer receiver and RFI processing incorporated in it to identify and understand interference.

2. REGIONAL IMPACT OF THE RFI

The best estimate for the location of the interference emitter based on localization algorithms from SMOS [1,2] and SMAP [3] is close to 30° 17'11" N, 119° 07'42" E, east of the city of Hangzhou.

Figure 1 illustrates the regional impact of the interference on SMAP measurements. It shows the maximum level (peak-hold) of antenna temperature observed by SMAP over the five days period from July 2 through July 7, 2020. The pin identifies the estimated location of the source. Particularly noticeable is the spatial effect of the RFI (appearing in yellow color) South of the emitter, reaching far beyond the transmitter itself. The diffuse spread of the signal is probably due to radiation entering the radiometer antenna though its side lobes and has the potential to corrupt science measurement even when the antenna points at positions other than the source of the RFI.

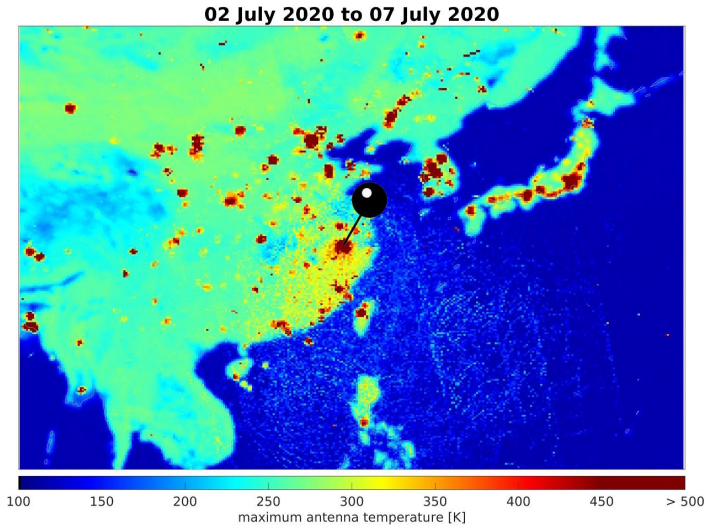

Figure 1: Peak-hold map of SMAP antenna temperature.

3. ANALYSIS OF RADIOMETER MEASUREMENTS

The radiometer on the Soil Moisture Active/Passive (SMAP) observatory operates in the protected spectrum window centered at 1.413 GHz and employs a conically

scanning antenna oriented at a fixed look angle of 35.5° with respect to the spacecraft scan axis (nadir) which corresponds to approximately 40° incidence angle at the surface [4,5] .

The fundamental datum of the SMAP radiometer is a measurement of emission from the Earth with an integration time of 0.3 ms and bandwidth of 24 MHz repeated every 0.35 ms. The 0.3 ms samples are grouped into "packets" of 4 samples (1.4 ms long with 1.2 ms of integration time). In addition to the science data, the data is available as a sequence of the individual 0.3 ms samples called "fullband" data, and also as "subband" data in which each packet is divided into 16 frequency channels each 1.5 MHz wide and reported as a function of time (once per packet). The RFI detection algorithm is applied to both the fullband and subband data streams [5].

3.1. Fullband Data

Figure 2 shows the antenna temperature before RFI filtering (i.e., detection and removal of RFI-affected samples) in V-polarization measured during a descending pass on July 7, 2020. The data appear as large circles (the antenna scans) composed of colored dots at the locations where the individual samples antenna temperature were acquired. Note the clustering of RFI (red dots) in the vicinity of the strong RFI source (circle). There are other sources of RFI in these figures, but they appear more concentrated and not to cover as extensive an area. Also, the interference source located in the position marked by the black circle affects the measurements at regular intervals, which is not the case for the other instances of interference.

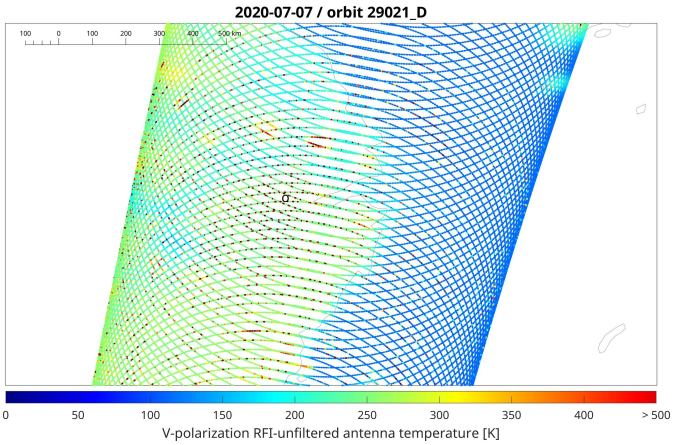

Figure 2: Map of antenna temperature along scans.

Figure 3 shows the temporal history of the samples (full band data) for a scan on July 5, 2020 that was impacted by the RFI. The RFI occurs in repetitive pulses suggestive of a radar, with amplitudes modulated by the SMAP antenna gain pattern as the antenna pointing approaches the source position and then moves away. The signal increases, reaches saturation at about 2,000 K and then decreases in amplitude as the antenna scans away. This behavior is suggestive of signals associated with radar systems for air traffic control and surveillance.

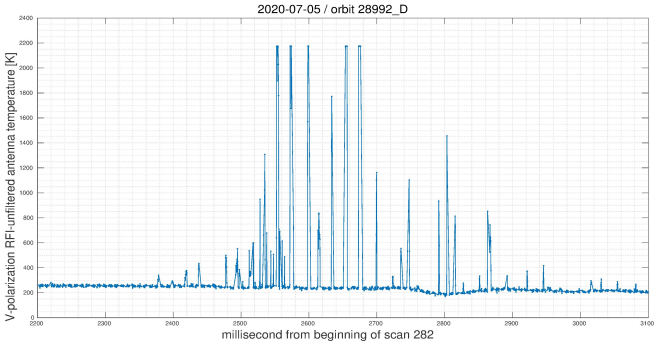

Figure 3: Temporal behavior of RFI (fullband data).

3.2. Subband Data

An analysis of the individual subband channels as in section 3.1 yields similar conclusions in terms of temporal behavior. However, the RFI appears to be not distributed evenly across the radiometer bandwidth, but concentrated only in one or two frequency channels. As an example, the distribution of RFI detected in the region affected by the interference source is shown in Figure 4 for the pass in Figure 2.

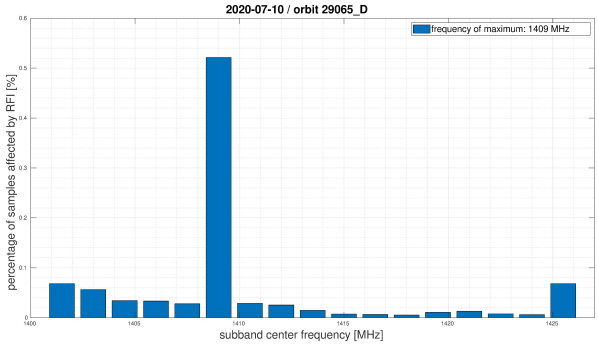

Figure 4: Frequency of the RFI based on subband data.

The offending transmission appears narrow-band and around 1409 MHz for this particular pass, however the distribution of observed interference power among frequency channels changes with time. This is illustrated in Figure 5, which shows the frequency with maximum amplitude as a function of the day of the measurement for

the period July 2-13. The possibility of this interference being caused by second harmonic emission of a transmitter around 750 MHz is extremely low because the 694-790 MHz band is allocated to the Broadcasting and Mobile services, which would not produce impulsive RFI. However, systems are permitted operation in the adjacent band 1350-1.400 GHz, and this suggests that the source of RFI is a surveillance radar that is involuntarily operating outside the allowed band perhaps due to a malfunction affecting the transmitted frequency.

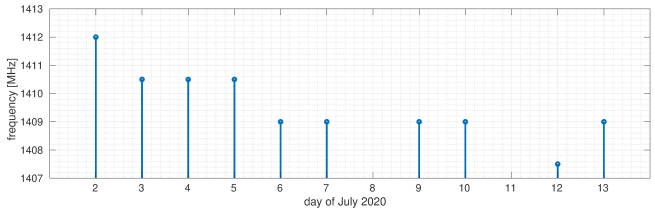

Figure 5: Evolution of the RFI frequency with time.

4. OTHER RESULTS

Based on the measurements acquired close to the source between July 2 and 13, 2020, the RFI signal appears to have the following characteristics:

- pulse-like time behavior with pulse width around 5-8 ms;
- pulse repetition time around 25-30 ms;
- bandwidth around 1.5-2.0 MHz;
- frequency that varies on the time scale of a few days.

An investigation of the directionality of the source has also been performed, that shows that the source is emitting toward the South-East direction.

5. CONCLUSIONS

A well-defined strong source of interference in China has been investigated using the tools of the SMAP radiometer specifically designed for detection of RFI. The results indicate that the emitter is most likely a radar and provide an indication of the characteristics of the radar pulses and the frequency of the side band entering the protected spectral window at 1.413 GHz.

This study also illustrates the potential of the processing incorporated in the SMAP radiometer to not only identify RFI but also to help understand the interference. Analyses of RFI sources such as the one provided in this paper can provide information to contribute to the enforcement of international radio regulations and help design future radiometer systems to better protect themselves from interference.

REFERENCES

[1] Oliva, R., Nieto, S. and Félix-Redondo, F., 2013. RFI detection algorithm: Accurate geolocation of the interfering sources in SMOS images. *IEEE Transactions on Geoscience and Remote Sensing*, 51(10), pp.4993-4998.

[2] Soldo, Y., Cabot, F., Khazaal, A., Miernecki, M., Słomińska, E., Fieuzal, R. and Kerr, Y.H., 2014. Localization of RFI sources for the SMOS mission: A means for assessing SMOS pointing performances. *IEEE Journal of Selected Topics in Applied Earth Observations and Remote Sensing*, 8(2), pp.617-627.

[3] Yan Soldo, Paolo de Matthaeis and David M. Le Vine, "Localization of L-band RFI sources from SMAP data", 32nd URSI GASS, Montreal, 19-26 August 2017.

[4] D. Entekhabi *et al*., "The Soil Moisture Active Passive (SMAP) Mission," *Proceedings of the IEEE*, vol. 98, no. 5, pp. 704-716, May 2010.

[5] Piepmeier, J.R., Johnson, J.T., Mohammed, P.N., Bradley, D., Ruf, C., Aksoy, M., Garcia, R., Hudson, D., Miles, L. and Wong, M., 2014. Radio-frequency interference mitigation for the soil moisture active passive microwave radiometer. *IEEE Transactions on Geoscience and Remote Sensing*, 52(1), pp.761-775.